Observation and characterization of the smallest borospherene, B_{28}^- and B_{28}

Ying-Jin Wang, Ya-Fan Zhao, Wei-Li Li, Tian Jian, Qiang Chen, Xue-Rui You, Ting Ou, Xiao-Yun Zhao, Hua-Jin Zhai' , Si-Dian Li' , Jun Li' , and Lai-Sheng Wang'

Citation: The Journal of Chemical Physics **144**, 064307 (2016); doi: 10.1063/1.4941380
View online: http://dx.doi.org/10.1063/1.4941380
View Table of Contents: http://aip.scitation.org/toc/jcp/144/6
Published by the American Institute of Physics

Observation and characterization of the smallest borospherene, B_{28}^- and B_{28}

Ying-Jin Wang,[1] Ya-Fan Zhao,[2] Wei-Li Li,[3] Tian Jian,[3] Qiang Chen,[1] Xue-Rui You,[1] Ting Ou,[1] Xiao-Yun Zhao,[1] Hua-Jin Zhai,[1,4,a)] Si-Dian Li,[1,a)] Jun Li,[2,a)] and Lai-Sheng Wang[3,a)]

[1]*Nanocluster Laboratory, Institute of Molecular Science, Shanxi University, Taiyuan 030006, China*
[2]*Department of Chemistry and Key Laboratory of Organic Optoelectronics and Molecular Engineering of Ministry of Education, Tsinghua University, Beijing 100084, China*
[3]*Department of Chemistry, Brown University, Providence, Rhode Island 02912, USA*
[4]*State Key Laboratory of Quantum Optics and Quantum Optics Devices, Shanxi University, Taiyuan 030006, China*

(Received 7 December 2015; accepted 11 January 2016; published online 8 February 2016)

Free-standing boron nanocages or borospherenes have been observed recently for B_{40}^- and B_{40}. There is evidence that a family of borospherenes may exist. However, the smallest borospherene is still not known. Here, we report experimental and computational evidence of a seashell-like borospherene cage for B_{28}^- and B_{28}. Photoelectron spectrum of B_{28}^- indicated contributions from different isomers. Theoretical calculations showed that the seashell-like B_{28}^- borospherene is competing for the global minimum with a planar isomer and it is shown to be present in the cluster beam, contributing to the observed photoelectron spectrum. The seashell structure is found to be the global minimum for neutral B_{28} and the B_{28}^- cage represents the smallest borospherene observed to date. It is composed of two triangular close-packed B_{15} sheets, interconnected via the three corners by sharing two boron atoms. The B_{28} borospherene was found to obey the $2(n+1)^2$ electron-counting rule for spherical aromaticity. © *2016 AIP Publishing LLC.* [http://dx.doi.org/10.1063/1.4941380]

I. INTRODUCTION

Since the discovery of the C_{60} buckminsterfullerene,[1] a family of carbon cages, generally known as fullerenes,[2] was discovered with C_{20} as the smallest possible fullerene. Even though the C_{20} fullerene was not the most stable form, competing as the global minimum with a quasi-planar bowl-shaped C_{20} and a monocyclic C_{20} ring,[3] it was observed experimentally and characterized[4] by photoelectron spectroscopy (PES) of C_{20}^-. There have been interests in fullerene-like cages made of other elements. However, only a few have been observed experimentally, including the Au_{16}^- golden cage,[5] the Sn_{12}^{2-} stannaspherene,[6] and the Pb_{12}^{2-} plumaspherene.[7] Boron, carbon's lighter neighbor, is the most obvious candidate to search for fullerene-type structures because of the strong B−B bond, which is only slightly weaker than a C−C bond. A B_{80} all-boron fullerene was proposed as a stable structure,[8] constructed by filling a boron atom to each of the 20 hexagons of a C_{60}-like B_{60} to compensate for boron's electron deficiency. Although the B_{80} fullerene cage was proved to be a much higher energy isomer,[9–13] recently the first all-boron fullerene, dubbed borospherene, has been observed and characterized for the 40-atom boron cluster.[14] The B_{40}^- anion was found to consist of two competing low-lying isomers, a quasi-planar structure and an unprecedented cage structure, consisting of four heptagons, two hexagons, and forty-eight B_3 triangles. For neutral B_{40}, the borospherene cage was found to be the overwhelming global minimum with a large energy gap between its highest occupied (HOMO) and lowest unoccupied (LUMO) molecular orbitals. There is evidence that there may exist a family of borospherenes.[15–17] However, the smallest borospherene is still not known.

Over the past decade, the structures and bonding of size-selected boron clusters have been systematically characterized experimentally and theoretically up to B_{27}^- using PES[18–21] and up to B_{25}^+ using ion mobility.[22] The anionic clusters up to B_{27}^- were all planar (2D), while there was a planar to tubular transition at B_{16}^+ for the cationic cluster. Beyond the B_{27}^- cluster, the B_{30}^-, B_{35}^-, and B_{36}^- clusters have all been found to be 2D with hexagonal vacancies,[23–25] providing indirect experimental evidence for the viability of monolayer-thin boron sheets[26] or borophenes,[25] whereas B_{39}^- has been found to be a chiral borospherene[15] similar to B_{40}^-. Recently, a computational study on B_{28} was reported,[27] suggesting that it forms the smallest all-boron cage with a distorted seashell shape of C_1 symmetry as the global minimum for both the neutral and anion.

Here, we report a joint PES and theoretical study on B_{28}^- and B_{28}. We found that the global minimum of B_{28}^- is a 2D structure with a buckled close-packed triangular lattice, whereas a seashell-like cage with C_2 symmetry is competing for the global minimum among three low-lying isomers, only 0.05 eV higher in energy than the 2D global minimum and 0.03 eV lower in energy than another 2D isomer with a hexagonal vacancy. The global minimum 2D structure was mainly responsible for the measured photoelectron spectrum of B_{28}^-, whereas concrete experimental evidence was observed

a)Electronic addresses: hj.zhai@sxu.edu.cn; lisidian@sxu.edu.cn; junli@tsinghua.edu.cn; and lai-sheng_wang@brown.edu

for the seashell cage isomer as a minor species in the cluster beam. In the neutral, the seashell-like B_{28} borospherene was found to be the global minimum with a similar structure as the B_{28}^- anion and also with C_2 symmetry. The B_{28}^- and B_{28} systems are similar to B_{40}^- and B_{40}, where a 2D structure was found to be the global minimum in the anion with the B_{40}^- borospherene as a close-lying isomer, whereas in the neutral the B_{40} borospherene was by far the most stable structure.[14]

II. EXPERIMENTAL METHOD

The experiment was carried out using a magnetic-bottle PES apparatus equipped with a laser vaporization source, details of which can be found elsewhere.[28] Briefly, negatively charged boron clusters were produced using an isotopically-enriched ^{10}B (96%) disk target. Nascent clusters were entrained by a He carrier gas containing 5% Ar and underwent a supersonic expansion to form a collimated and vibrationally cold cluster beam. The size distribution and the cooling were controlled by the time delay between the pulsed valve and the vaporization laser and by the resident time of the clusters in the nozzle.[29,30] The anionic clusters were analyzed using a time-of-flight mass spectrometer. The B_{28}^- clusters were mass-selected and decelerated before being intercepted by a detachment laser beam. The photodetachment experiment was conducted at 193 nm (6.424 eV) from an ArF excimer laser. Photoelectrons were collected at nearly 100% efficiency by the magnetic bottle and analyzed in a 3.5 m long electron flight tube. The photoelectron spectrum was calibrated using the known spectrum of Au^- and the resolution of the apparatus was $\Delta E_k/E_k \approx 2.5\%$, that is, ~25 meV for 1 eV kinetic energy electrons.

III. THEORETICAL METHODS

We searched for the global minimum and low-lying isomers of B_{28}^- using both the Minima Hopping (MH)[31] and Basin Hopping (BH)[32] methods, as well as manual structural constructions, at the density-functional theory (DFT) level. Low-lying structures were then fully optimized and their relative energies evaluated at the PBE0 level[33] with the 6-311+G* basis set.[34] Vibrational frequencies were calculated to ensure that each isomeric structure presented was a true minimum on the potential energy surface. To obtain more accurate relative energies, the top five lowest-lying isomers of B_{28}^- at PBE0/6-311+G* were further refined at the single-point coupled-cluster level with single, double, and perturbative triple excitations [CCSD(T)]/6-311G*//PBE0/6-311+G*.[35–37] For comparison with experimental PES data, vertical detachment energies (VDEs) of the lowest four isomers at the CCSD(T) level were calculated using the PBE0/6-311+G* method. The first VDE was calculated as the difference in energy between the anionic ground state and the corresponding neutral state at the anion geometry, and then vertical excitation energies of the neutral species calculated at the time-dependent PBE0 (TD-PBE0) level[38] were added to the first VDE to approximate the second and higher VDEs. Chemical bonding analyses were performed using the adaptive natural density partitioning (AdNDP) method developed by Zubarev and Boldyrev[39] at the PBE0/6-31G level of theory. The AdNDP results were visualized using the Molekel 5.4.0.8 program.[40] The PBE0/6-311+G* calculations were done using the Gaussian 09 program[41] and the CCSD(T)/6-311G*//PBE0/6-311+G* calculations using the Molpro package.[42] Molecular structures and MOs were visualized using the GaussView 5.0.9 program.[43]

IV. EXPERIMENTAL RESULTS

The photoelectron spectrum of B_{28}^- at 193 nm is shown in Fig. 1(a). The spectrum is relatively congested and broad, in particular, beyond 4 eV, suggesting that multiple detachment transitions may contribute to each spectral band or multiple isomers may exist in the cluster beam and contribute to the observed spectrum. Major spectral features are labeled with letters (X, A– D) and the estimated VDEs are summarized in Table I, where they are compared with theoretical calculations. Band X should represent the transition from the ground state of the anion to that of the neutral of the dominant isomer. The ground state VDE is estimated to be 3.64 eV from band X. The adiabatic detachment energy (ADE) for the ground state transition is evaluated to be 3.44 eV from the onset of band X, which represents the electron affinity of the corresponding neutral B_{28}. Higher binding energy features, from A to D, represent transitions to excited states of the neutral and they are labeled for the sake of discussion, because of the broad spectral width and the expected overlaps of many transitions. The VDEs given in Table I are estimates, representing the averages of possible multiple detachment transitions. A very weak spectral feature, labeled as X′, is observed at the low binding energy side of the spectrum in Fig. 1(a). The intensity of band X′ is ~10% of that of band X and can be increased to about 20% relative to band X under hotter source conditions, suggesting that it originates from a minor isomer of B_{28}^- in the cluster beam. From band X′, we estimate an ADE of 3.00 eV and a VDE of 3.05 eV for the minor isomer, as given in Table S1.[44]

V. THEORETICAL RESULTS

We used both the MH and BH methods to search for the global minimum and low-lying isomers of B_{28}^- at the DFT level. More than 3100 stationary points on the potential energy surface were examined for B_{28}^- at low levels of theory. Ninety-one structures were found at the PBE0 level within 2 eV of the global minimum, as given in Fig. S1.[44] The top five structures were refined at the CCSD(T) level of theory, as shown in Fig. 2. At both the PBE0 and CCSD(T) levels of theory, a close-packed 2D structure **I** (C_2, ^{2}A) was found to be the global minimum for B_{28}^-, which is comprised of a 16-atom periphery with 12 interior atoms in a buckled triangular lattice. The second isomer **II** (C_2,^{2}A) is a three-dimensional (3D) seashell-like cage isomer, which is only 0.05 eV higher in energy than the global minimum at the CCSD(T) level. Both isomers **I** and **II** are chiral and their enantiomers are shown in

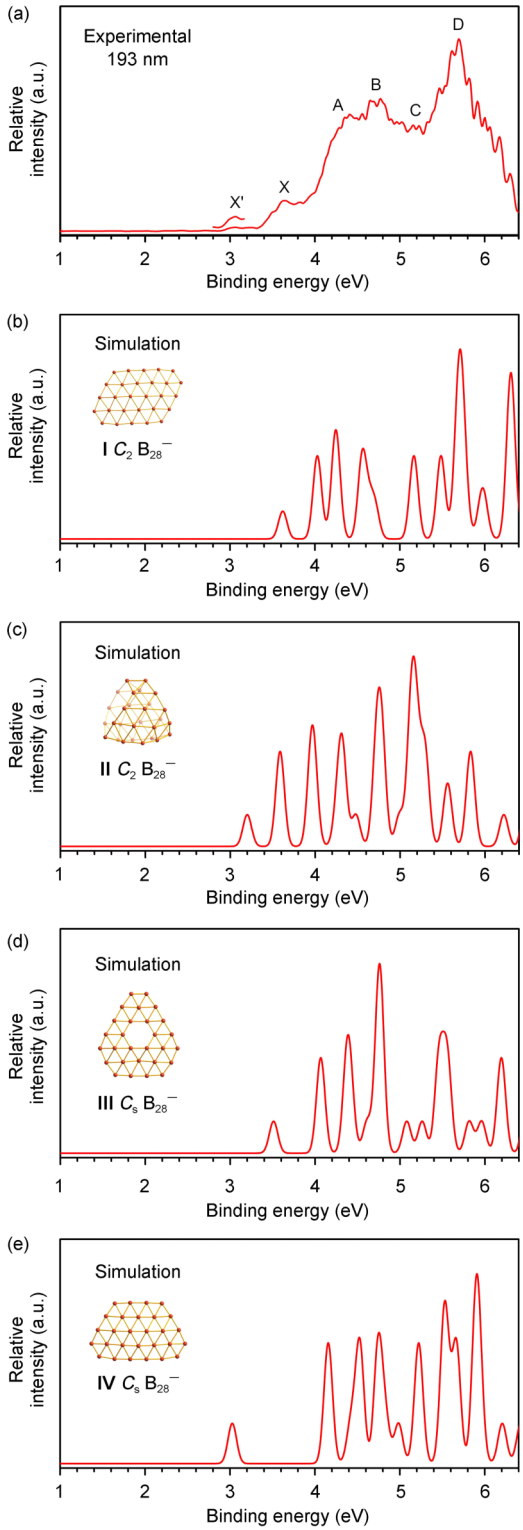

FIG. 1. The photoelectron spectrum of B_{28}^- and comparison with simulated spectra. (a) The photoelectron spectrum of B_{28}^- at 193 nm (6.424 eV). The X′ band is enlarged by three times to show the details. (b)-(e) Simulated spectra based on isomers **I**, **II**, **III**, and **IV** (see Figure 2) at the time-dependent PBE0/6-311+G* level. The simulations were done by fitting the calculated VDEs with unit-area Gaussian functions of 0.1 eV half-width.

Fig. 3, where more structural details are also given. The cage isomer **II** consists of two quasi-planar B_{15} triangular sheets fused together by sharing two corner atoms at the bottom and via a B_2 twist at the top corner. The seashell cage contains two heptagons on the waist and a hexagon at the bottom, all formed between the two B_{15} sheets. It has a height of 5.0 Å, a width of 5.5 Å in the bottom, and a thickness of 4.1 Å, which has enough space to host an endohedral atom ("seashell with a pearl").

The third isomer **III** (C_s,^{2}A′) containing a hexagonal vacancy is only 0.08 eV above the global minimum at the CCSD(T) level (Fig. 2(a)). The global minimum of B_{27}^-, in fact, contained a hexagonal vacancy[21] and isomer **III** of B_{28}^- is related to the hexagonal B_{36} (which can be reached by adding a row of four boron atoms on each side of isomer **III**).[25] Isomer **IV** (C_s,^{2}A′) also with a buckled triangular lattice like the global minimum, but with a slightly different atomic arrangement, is substantially higher in energy (0.26 eV above the global minimum at the CCSD(T) level). A double-ring isomer **V** (D_{2d},^{2}A$_1$) is found to be 0.38 eV above the global minimum at the CCSD(T) level. Among the 91 isomers presented in Fig. S1,[44] 72 are quasi-planar, 18 are cage-like, and one is tubular, suggesting an interesting competition between the cages and 2D structures at this size. In a recent computational study on B_{28}^- by Zhao *et al.*,[27] a seashell-like cage with C_1 symmetry was reported as the global minimum with two low-lying isomers similar to isomers **IV** and **V** in Fig. 2(a), but isomers **I** and **III** were missed. The C_1 cage by Zhao *et al.* looks identical to the current cage isomer **II** in Fig. 2. Since we observed no such C_1 cage in our low-lying isomers (all were confirmed to be true minima by frequency calculations), we suspected that the symmetry might have been misidentified by Zhao *et al.* In another computational study on B_{28}^- by Tai and Nguyen,[45] similar isomers and energetics as isomers **I**, **III**, **IV**, and **V** were reported, but the seashell-like cage isomer was missed.

For neutral B_{28}, the same set of low-lying isomers with very similar structures to the anions were found, as shown in Fig. 2(b), but the energetic ordering has changed. Remarkably, the seashell-like borospherene cage (**VI**, C_2,^{1}A) becomes the global minimum at the CCSD(T) level. The second isomer **VII** (C_s,^{1}A′), corresponding to isomer **IV** of the anion, is 0.18 eV higher in energy at the CCSD(T) level. Isomers **VIII**, **IX**, and **X** are all much higher in energy for neutral B_{28} at the CCSD(T) level. Isomer **X**, corresponding to the global minimum of B_{28}^-, is 0.51 eV higher above the cage global minimum for the neutral. The first three isomers of neutral B_{28} reported by Zhao *et al.*[27] are similar to isomers **VI**, **VII**, and **VIII** in Fig. 2(b), whereas the first four isomers reported by Tai and Nguyen[45] are similar to isomers **VII**–**X**, again missing the global minimum seashell cage **VI**.

VI. COMPARISON BETWEEN EXPERIMENT AND THEORY

The relative energies of isomers **I**, **II**, and **III** of B_{28}^- are so close and the true global minimum can only be determined by comparison with the experiment. All these isomers might coexist in the experiment, whereas isomers **IV** and **V** can be safely ruled out on the basis of the energetics. The calculated VDEs for isomers **I**–**IV** at the TD-PBE0/6-311+G* level are given in Tables I and S1–S3,[44] while the simulated spectra using the calculated VDEs are compared

TABLE I. Comparison of the experimental VDEs (in eV) of B_{28}^- with the calculated VDEs at the time-dependent PBE0/6-311+G* (TD-PBE0) level for isomer **I** (C_2, ^{2}A).

Feature	VDE (expt.)	Final state and electronic configuration	VDE (TD-PBE0)[a]
X′	3.05(7)[b]		
X	3.64(6)[b]	^{1}A {…17a^2 18a^2 17b^2 18b^2 19a^2 20a^2 19b^2 21a^2 20b^2 21b^2 22a^0}	3.61
		^{3}B {…17a^2 18a^2 17b^2 18b^2 19a^2 20a^2 19b^2 21a^2 20b^2 21b^1 22a^1}	4.02
A	~4.4	^{3}B {…17a^2 18a^2 17b^2 18b^2 19a^2 20a^2 19b^2 21a^2 20b^1 21b^2 22a^1}	4.23
		^{1}B {…17a^2 18a^2 17b^2 18b^2 19a^2 20a^2 19b^2 21a^2 20b^2 21b^1 22a^1}	4.25
B	~4.7	^{3}A {…17a^2 18a^2 17b^2 18b^2 19a^2 20a^2 19b^2 21a^1 20b^2 21b^2 22a^1}	4.55
		^{1}B {…17a^2 18a^2 17b^2 18b^2 19a^2 20a^2 19b^2 21a^2 20b^1 21b^2 22a^1}	4.64
		^{1}A {…17a^2 18a^2 17b^2 18b^2 19a^2 20a^2 19b^2 21a^1 20b^2 21b^2 22a^1}	4.70
C	~5.2	^{3}B {…17a^2 18a^2 17b^2 18b^2 19a^2 20a^2 19b^1 21a^2 20b^2 21b^2 22a^1}	5.16
D	5.70(6)	^{3}A {…17a^2 18a^2 17b^2 18b^2 19a^2 20a^1 19b^2 21a^2 20b^2 21b^2 22a^1}	5.47
		^{1}B {…17a^2 18a^2 17b^2 18b^2 19a^2 20a^2 19b^1 21a^2 20b^2 21b^2 22a^1}	5.65
		^{3}B {…17a^2 18a^2 17b^2 18b^1 19a^2 20a^2 19b^2 21a^2 20b^2 21b^2 22a^1}	5.69
		^{3}A {…17a^2 18a^2 17b^2 18b^2 19a^1 20a^2 19b^2 21a^2 20b^2 21b^2 22a^1}	5.72
		^{1}A {…17a^2 18a^2 17b^2 18b^2 19a^2 20a^1 19b^2 21a^2 20b^2 21b^2 22a^1}	5.76
		^{1}B {…17a^2 18a^2 17b^2 18b^1 19a^2 20a^2 19b^2 21a^2 20b^2 21b^2 22a^1}	5.94
		^{1}A {…17a^2 18a^2 17b^2 18b^2 19a^1 20a^2 19b^2 21a^2 20b^2 21b^2 22a^1}	5.99
		^{3}B {…17a^2 18a^2 17b^1 18b^2 19a^2 20a^2 19b^2 21a^2 20b^2 21b^2 22a^1}	6.30
		^{3}A {…17a^2 18a^1 17b^2 18b^2 19a^2 20a^2 19b^2 21a^2 20b^2 21b^2 22a^1}	6.30

[a]Calculated at the TD-PBE0/6-311+G* level.
[b]Adiabatic detachment energy: 3.00 ± 0.07 eV for X′ and 3.44 ± 0.06 eV for X.

with the experimental spectrum in Fig. 1. The stimulated spectrum of isomer **I** (Fig. 1(b)) agrees well with the major PES features (X, A–D). In particular, the calculated first VDE from electron detachment from the HOMO, 3.61 eV (Table I), is in excellent agreement with the measured VDE of band X (3.64 eV). However, the gap between 4.7 and 5.1 eV in the simulated spectrum of isomer **I** does not agree with the experiment, suggesting contributions from other isomers.

The calculated first VDE for the seashell cage structure **II** is 3.19 eV (Table S1),[44] which is in good agreement with the minor band X′ at 3.05 eV. Most of the higher binding energy VDEs of isomer **II** overlap with those from isomer **I**, but the features in the 4.7–5.1 eV range are consistent with the experimental spectrum. The simulated spectral features of isomer **III** overlap with those from isomers **I** and **II**, but it cannot be ruled out on the bases of its energetics. However, if isomer **II** only made a 10% contribution, the contribution from isomer **III** was expected to be even smaller or negligible. The calculated first VDE of isomer **IV** is 3.02 eV, which is in good agreement with the minor band X′. However, this isomer is significantly higher-lying and is not expected to be populated in the experiment. The overall good agreement of the experimental spectrum with the combined simulated

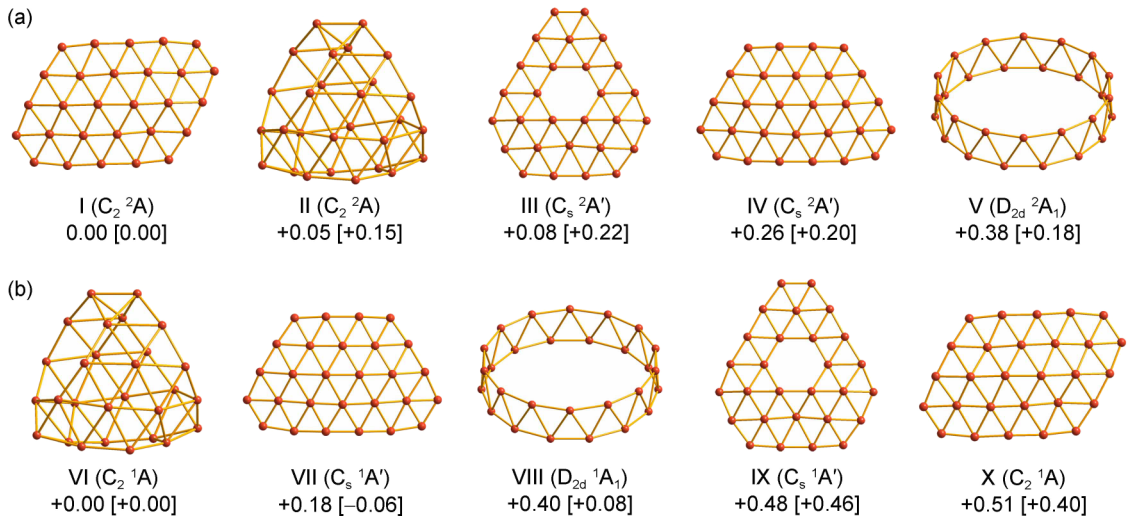

FIG. 2. The optimized structures for B_{28}^- and B_{28}. (a) The global minimum (**I**) and four low-lying isomers (**II**–**V**) of B_{28}^- at the PBE0/6-311+G* level. (b) The global minimum (**VI**) and four low-lying isomers (**VII**–**X**) of B_{28} at the PBE0/6-311+G* level. Relative energies are given in eV at CCSD(T)/6-311G*//PBE0/6-311+G* and PBE0/6-311+G* (in square brackets) levels. The energies at the PBE0 level are corrected for zero-point energies.

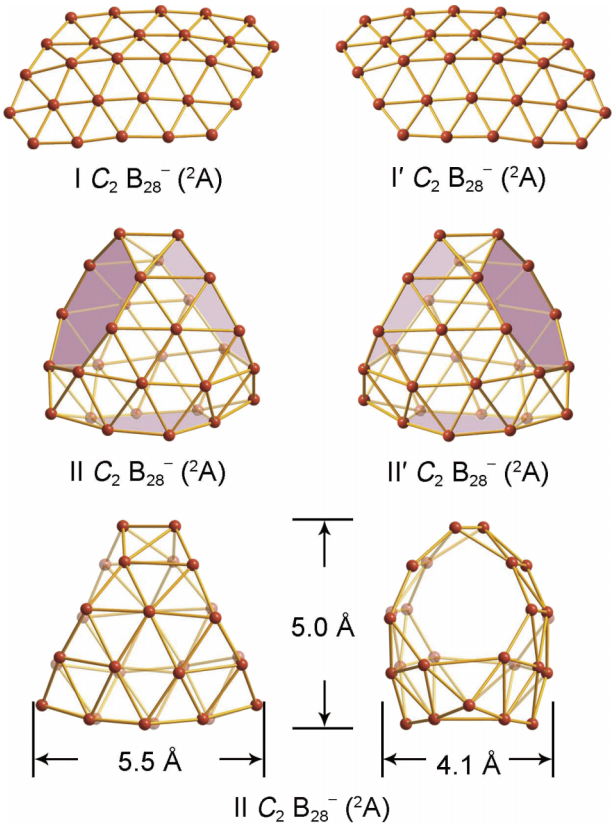

FIG. 3. The enantiomers of the chiral global minimum and the seashell isomer **II** of B_{28}^- and the dimensions of the seashell cage at the PBE0/6-311+G* level. The two B_7 rings on the waist and the B_6 ring at the bottom of the seashell isomer are shaded for easier viewing.

spectra of isomers **I** and **II** provides considerable credence for the 2D global minimum of B_{28}^- and the cage isomer **II**.

VII. DISCUSSION

A. Chemical bonding analyses of the 2D global minimum of B_{28}^-

The global minimum of B_{28}^- has a buckled close-packed triangular lattice. The maximum out-of-plane distortion of the inner boron atom is about 1.1 Å, similar to that found previously in the buckled B_{22}^- triangular-lattice structure (0.93 Å).[46] Since the global minimum of B_{28}^- is open-shell with an unpaired electron, we used a planarized closed-shell B_{28}^{2-} with C_{2h} symmetry for the purpose of chemical bonding analyses. The C_{2h} B_{28}^{2-} was found to possess ten delocalized π orbitals, which are reminiscent of the polycyclic aromatic hydrocarbon, dicyclopenta[cd,jk]pyrene ($C_{20}H_{10}$), as shown in Fig. S2.[44] We further explored the bonding analogy between the C_{2h} B_{28}^{2-} and $C_{20}H_{10}$ by electron localization function (ELF) and AdNDP analyses, as shown in Fig. 4. The similarity in the π bonding between the two systems is revealed even more vividly. Two representations of the π bonding pattern may be obtained via AdNDP: the Kekule type or the Clar type. The Clar representation shown in Fig. 4 gives better occupation numbers (ONs). The Kekule representation is displayed in Fig. S3,[44] where the σ bonding is also presented.

B. Chemical bonding in the seashell B_{28}^- and B_{28} cages

We also analyzed the chemical bonding in the seashell isomer using ELF and AdNDP, as shown in Fig. 5. Since B_{28}^- is open shell, we focus on the closed-shell neutral seashell B_{28}. The ELFσ and ELFπ are illustrated in Fig. 5(a). The ELFσ pattern suggests the dominance of three-center σ bonds on the cage surface, consistent with the AdNDP results shown in Fig. 5(b). There are thirty-eight B_3 triangles on the B_{28} cage, sixteen from each B_{15} sheets plus six from the interface of the two B_{15} sheets. However, there are only thirty-two 3-center-2-electron (3c-2e) bonds. Unlike the B_{40} borospherene,[14] not all B_3 triangles have a 3c-2e bond in the B_{28} cage. In addition, a 12c-2e σ bond is found (Fig. 5(b)), which contains electron density from the six B_3 triangles that do not have a 3c-2e bond, suggesting that the seashell B_{28} cage is electron-deficient in the σ framework.

The ELFπ pattern suggests nine π bonds (Fig. 5(a)), also consistent with the AdNDP results shown in Fig. 5(c). Each of the B_{15} sheets has three 5c-2e delocalized π bonds. Very interestingly, the three remaining π bonds are delocalized at the three corner sites, where the two B_{15} sheets are connected, resulting in fairly uniform π bonding on the seashell cage surface. Furthermore, the nine delocalized π bonds with a total of 18 π electrons in the B_{28} seashell cage conform to the $2(n+1)^2$ π electron-counting rule for spherical aromaticity found in fullerenes (n = integers, 2 in this case).[47] Thus, the seashell B_{28} can be considered to be aromatic. Indeed, the calculated nuclear-independent chemical shift (NICS) value,[48] an indicator of aromaticity, at the cage center of B_{28} amounts to −39.97 ppm at PBE0/6-311+G*, which is highly negative and consistent with its spherical aromaticity.

C. The seashell B_{28}^-: The smallest borospherene?

The current B_{28}^- and B_{28} cages are similar in shape and construction to those reported by Zhao *et al.*,[27] even though their cages had no symmetry (C_1). Clearly, the global minimum of B_{28}^- was also missed in that study. Tai and Nguyen did identify the global minimum of B_{28}^-, but they missed the seashell cage isomer in the anion and the cage global minimum for the neutral.[45] These medium-sized boron clusters are fairly complicated. Only the most careful global searches in combination with experiment can yield the global minimum with confidence. Since the discovery of the B_{40}^- and B_{40} borospherenes, the B_{39}^- cluster has been confirmed to be a chiral borospherene.[15] Computationally, B_{38} has been reported to have a cage global minimum[16] or as a low-lying isomer,[49] whereas B_{41}^+ has been shown to be a cage similar to the B_{40} borospherene.[17] Hence, there seems to be a family of borospherenes. Experimentally, all boron clusters up to B_{27}^- have been shown to have 2D global minima.[21] Hence, the seashell B_{28}^- is the smallest borospherene observed experimentally, even though it is not the global minimum. With 2 heptagons, 1 hexagon, and 38 triangles on the surface, the B_{28}^- borospherene follows the Euler's rule: E (67 edges) = F (38 triangular + 1 hexagonal + 2 heptagonal faces) + V (28 vertices) − 2.

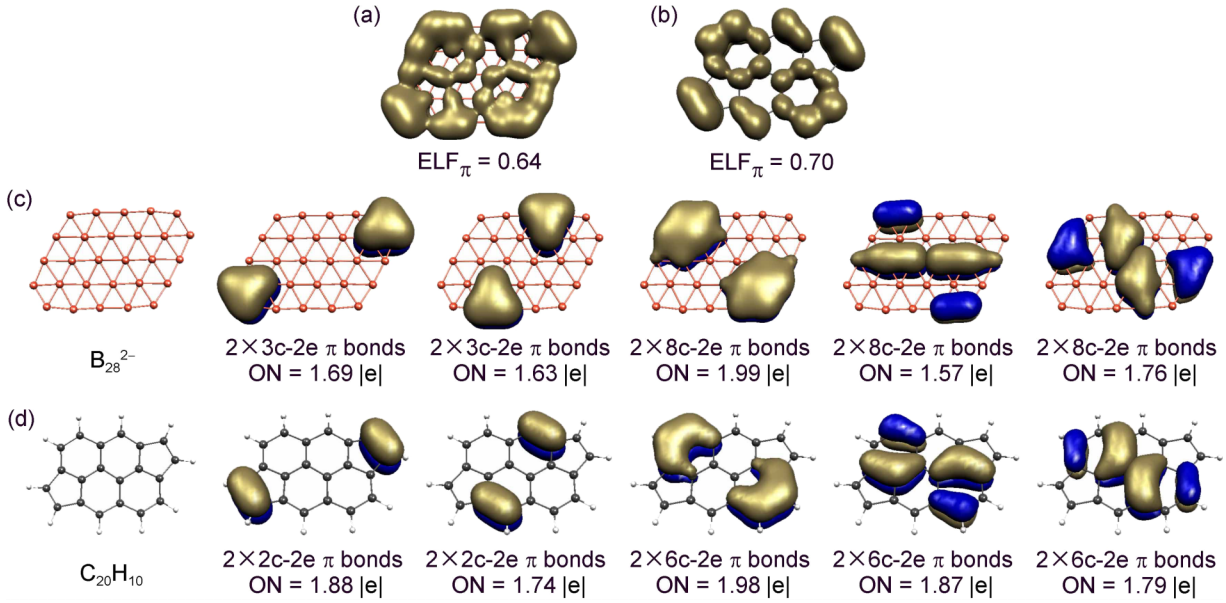

FIG. 4. Chemical bonding analyses for the quasi-planar global minimum of B_{28}^- using the planarized closed-shell C_{2h} B_{28}^{2-}. (a) The ELFπ for B_{28}^{2-}. (b) The ELFπ for $C_{20}H_{10}$. (c) The Clar type π bonds for B_{28}^{2-} at the PBE0/6-31G level using AdNDP analyses. (d) The Clar type π bonds for $C_{20}H_{10}$ at the PBE0/6-31G* level using AdNDP analyses. The occupation numbers (ONs) are shown.

The structures of the borospherene family mainly contain B_3 triangles, which are the dominating bonding units in boranes and all the boron allotropes, along with hexagons and heptagons. These structural features, due to the electron deficiency of boron, are different from fullerenes, which exclusively formed from pentagons and hexagons as a result of sp^2 hybridization. Hence, borospherenes have less smooth surfaces, mainly because of the presence of the heptagons. The structural evolution of boron clusters is also complicated. The B_{28}^- cluster is not the onset of borospherene, since several larger clusters, in particular, B_{30}^-, B_{35}^-, and B_{36}^- have been confirmed to have 2D global minimum.[23–25] More borospherenes will undoubtedly be uncovered, but they cannot be predicted because of the electron deficient nature of boron and its odd valence electron count. Both the right number of electrons and suitable geometric structures are necessary to allow a truly stable borospherene cage.

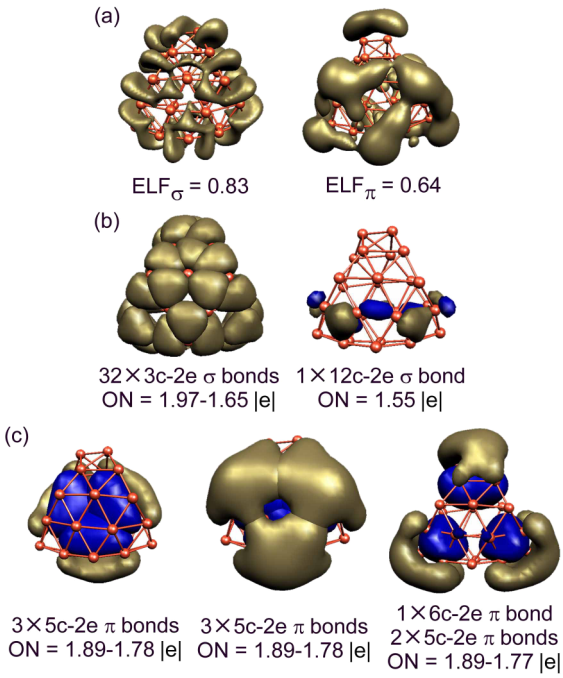

FIG. 5. Chemical bonding analyses for the seashell-like B_{28} borospherene. (a) The ELFσ and ELFπ. (b) The σ bonding using AdNDP analyses. (c) The π bonding using AdNDP analyses. The occupation numbers (ONs) are shown.

VIII. CONCLUSIONS

A joint photoelectron spectroscopy and quantum chemistry study has been carried out to investigate the structures and bonding of the B_{28}^- and B_{28} clusters. A low-lying seashell-like cage structure with C_2 symmetry was found to be only 0.05 eV above the global minimum, which is a planar structure with a close-packed and buckled triangular lattice. The seashell cage structure is composed of two quasi-planar triangular B_{15} sheets, interconnected at the three corners by sharing two boron atoms in two of the three corners. Both the cage structure and the planar B_{28}^- were observed experimentally with the cage isomer as a minor component in the cluster beam. A third planar structure with a hexagonal vacancy was also found theoretically to be only 0.08 eV above the global minimum. The π bonding in the planar global minimum was found to be similar to that of the dicyclopenta[cd,jk]pyrene ($C_{20}H_{10}$) polycyclic aromatic molecule. For the neutral B_{28} cluster, the seashell-like isomer was found to be the global minimum. Nine π bonds are found to distribute evenly over the cage surface and the π bonding conforms to the $2(n + 1)^2$ electron-counting rule for spherical aromaticity. The seashell-like B_{28}^- cage represents the smallest borospherene observed experimentally.

ACKNOWLEDGMENTS

This experimental work done at Brown University was supported by the US National Science Foundation (No. CHE-1263745). The theoretical work was supported by the National Natural Science Foundation of China (Nos. 21243004, 21373130, and 21573138), the National Key Basic Research Special Foundations (No. 2011CB932401), and the State Key Laboratory of Quantum Optics and Quantum Optics Devices (No. KF201402). H.J.Z. gratefully acknowledges Shanxi University for support via the start-up fund.

[1]H. W. Kroto, J. R. Heath, S. C. O'Brien, R. F. Curl, and R. E. Smalley, Nature **318**, 162 (1985).
[2]H. W. Kroto, Nature **329**, 529 (1987).
[3]Y. Jin, A. Perera, V. F. Lotrich, and R. J. Bartlett, Chem. Phys. Lett. **629**, 76 (2015).
[4]H. Prinzbach, A. Weiler, P. Landenberger, F. Wahl, J. Worth, L. T. Scott, M. Gelmont, D. Olevano, and B. V. Issendorff, Nature **407**, 60 (2000).
[5]S. Bulusu, X. Li, L. S. Wang, and X. C. Zeng, Proc. Natl. Acad. Sci. U. S. A. **103**, 8326 (2006).
[6]L. F. Cui, X. Huang, L. M. Wang, D. Y. Zubarev, A. I. Boldyrev, J. Li, and L. S. Wang, J. Am. Chem. Soc. **128**, 8390 (2006).
[7]L. F. Cui, X. Huang, L. M. Wang, J. Li, and L. S. Wang, J. Phys. Chem. A **110**, 10169 (2006).
[8]N. G. Szwacki, A. Sadrzadeh, and B. I. Yakobson, Phys. Rev. Lett. **98**, 166804 (2007); Erratum, **100**, 159901 (2008).
[9]D. L. V. K. Prasad and E. D. Jemmis, Phys. Rev. Lett. **100**, 165504 (2008).
[10]H. Li, N. Shao, B. Shang, L. F. Yuan, J. Yang, and X. C. Zeng, Chem. Commun. **46**, 3878 (2010).
[11]J. Zhao, L. Wang, F. Li, and Z. Chen, J. Phys. Chem. A **114**, 9969 (2010).
[12]S. De, A. Willand, M. Amsler, P. Pochet, L. Genovese, and S. Goedecker, Phys. Rev. Lett. **106**, 225502 (2011).
[13]F. Li, P. Jin, D. Jiang, L. Wang, S. B. Zhang, J. Zhao, and Z. Chen, J. Chem. Phys. **136**, 074302 (2012).
[14]H. J. Zhai, Y. F. Zhao, W. L. Li, Q. Chen, H. Bai, H. S. Hu, Z. A. Piazza, W. J. Tian, H. G. Lu, Y. B. Wu, Y. W. Mu, G. F. Wei, Z. P. Liu, J. Li, S. D. Li, and L. S. Wang, Nat. Chem. **6**, 727 (2014).
[15]Q. Chen, W. L. Li, Y. F. Zhao, S. Y. Zhang, H. S. Hu, H. Bai, H. R. Li, W. J. Tian, H. G. Lu, H. J. Zhai, S. D. Li, J. Li, and L. S. Wang, ACS Nano **9**, 754 (2015).
[16]J. Lv, Y. Wang, L. Zhu, and Y. Ma, Nanoscale **6**, 11692 (2014).
[17]Q. Chen, S. Y. Zhang, H. Bai, W. J. Tian, T. Gao, H. R. Li, C. Q. Miao, Y. W. Mu, H. G. Lu, H. J. Zhai, and S. D. Li, Angew. Chem., Int. Ed. **54**, 8160 (2015).
[18]A. N. Alexandrova, A. I. Boldyrev, H. J. Zhai, and L. S. Wang, Coord. Chem. Rev. **250**, 2811 (2006).
[19]W. Huang, A. P. Sergeeva, H. J. Zhai, B. B. Averkiev, L. S. Wang, and A. I. Boldyrev, Nat. Chem. **2**, 202 (2010).
[20]A. P. Sergeeva, I. A. Popov, Z. A. Piazza, W. L. Li, C. Romanescu, L. S. Wang, and A. I. Boldyrev, Acc. Chem. Res. **47**, 1349 (2014).
[21]W. L. Li, R. Pal, Z. A. Piazza, X. C. Zeng, and L. S. Wang, J. Chem. Phys. **142**, 204305 (2015).
[22]E. Oger, N. R. M. Crawford, R. Kelting, P. Weis, M. M. Kappes, and R. Ahlrichs, Angew. Chem., Int. Ed. **46**, 8503 (2007).
[23]W. L. Li, Y. F. Zhao, H. S. Hu, J. Li, and L. S. Wang, Angew. Chem., Int. Ed. **53**, 5540 (2014).
[24]W. L. Li, Q. Chen, W. J. Tian, H. Bai, Y. F. Zhao, H. S. Hu, J. Li, H. J. Zhai, S. D. Li, and L. S. Wang, J. Am. Chem. Soc. **136**, 12257 (2014).
[25]Z. A. Piazza, H. S. Hu, W. L. Li, Y. F. Zhao, J. Li, and L. S. Wang, Nat. Commun. **5**, 3113 (2014).
[26]H. Tang and S. Ismail-Beigi, Phys. Rev. Lett. **99**, 115501 (2007).
[27]J. Zhao, X. Huang, R. Shi, H. Liu, Y. Su, and R. B. King, Nanoscale **7**, 15086 (2015).
[28]L. S. Wang, H. S. Cheng, and J. Fan, J. Chem. Phys. **102**, 9480 (1995).
[29]L. S. Wang and X. Li, "Temperature effects in anion photoelectron spectroscopy of metal clusters," in *Clusters and Nanostructure Interfaces*, edited by P. Jena, S. N. Khanna, and B. K. Rao (World Scientific, River Edge, New Jersey, 2000), pp. 293–300.
[30]W. Huang and L. S. Wang, Phys. Rev. Lett. **102**, 153401 (2009).
[31]S. Goedecker, J. Chem. Phys. **120**, 9911 (2004).
[32]D. J. Wales and H. A. Scheraga, Science **285**, 1368 (1999).
[33]C. Adamo and V. Barone, J. Chem. Phys. **110**, 6158 (1999).
[34]R. Krishnan, J. S. Binkley, R. Seeger, and J. A. Pople, J. Chem. Phys. **72**, 650 (1980).
[35]J. Čížek, Adv. Chem. Phys. **14**, 35 (1969).
[36]G. D. Purvis III and R. J. Bartlett, J. Chem. Phys. **76**, 1910 (1982).
[37]K. Raghavachari, G. W. Trucks, J. A. Pople, and M. Head-Gordon, Chem. Phys. Lett. **157**, 479 (1989).
[38]R. Bauernschmitt and R. Ahlrichs, Chem. Phys. Lett. **256**, 454 (1996).
[39]D. Y. Zubarev and A. I. Boldyrev, Phys. Chem. Chem. Phys. **10**, 5207 (2008).
[40]U. Varetto, Molekel 5.4.0.8, Swiss National Supercomputing Center, Manno, Switzerland, 2009.
[41]M. J. Frisch, G. W. Trucks, H. B. Schlegel, G. E. Scuseria, M. A. Robb, J. R. Cheeseman, G. Scalmani, V. Barone, B. Mennucci, G. A. Petersson *et al.*, GAUSSIAN 09, Revision B.01, Gaussian, Inc., Wallingford, CT, 2009.
[42]H. J. Werner, P. J. Knowles, G. Knizia, F. R. Manby, M. Schütz, P. Celani, T. Korona, R. Lindh, A. Mitrushenkov, G. Rauhut *et al.*, MOLPRO, version 2012.1, a package of *ab initio* programs, 2012, see http://www.molpro.net.
[43]R. Dennington, T. Keith, and J. Millam, GaussView, version 5.0.9, Semichem, Inc., Shawnee Mission, KS, 2009.
[44]See supplementary material at http://dx.doi.org/10.1063/1.4941380 for a full set of the optimized low-lying structures, bonding analyses of the planar B_{28}^{2-}, computed VDEs for isomers **II-IV**, and the coordinates of isomers **I-V**.
[45]T. B. Tai and M. T. Nguyen, Phys. Chem. Chem. Phys. **17**, 13672 (2015).
[46]A. P. Sergeeva, Z. A. Piazza, C. Romanescu, W. L. Li, A. I. Boldyrev, and L. S. Wang, J. Am. Chem. Soc. **134**, 18065 (2012).
[47]A. Hirsch, Z. Chen, and H. Jiao, Angew. Chem., Int. Ed. **39**, 3915 (2000).
[48]P. v. R. Schleyer, C. Maerker, A. Dransfeld, H. Jiao, and N. J. v. E. Hommes, J. Am. Chem. Soc. **118**, 6317 (1996).
[49]T. B. Tai and M. T. Nguyen, Nanoscale **7**, 3316 (2015).